Comparison between Perturb & Observe Method and Incremental Conductance Method for Maximum Power Point Tracking of PV Module

A Dissertation submitted in fulfillment of the requirements for the Degree of

MASTER OF ENGINEERING

in

Power Systems

Submitted by

Rahul Tomar

Regd. No. : 801441021

Under the Guidance of

Dr. Prasenjit Basak

Assistant Professor, EIED

2016

Electrical and Instrumentation Engineering Department

Thapar University, Patiala

(Declared as Deemed-to-be-University u/s 3 of the UGC Act., 1956)

Post Bag No. 32, Patiala – 147004

Punjab (India)

DECLARATION

I hereby certify that the work which is presented in dissertation entitled, "Comparison between Perturb & Observe Method and Incremental Conductance Method for Maximum Power Point Tracking of PV Module", in fulfillment of the requirements for the award of the degree of Master of Engineering in Power Systems, submitted to Electrical & Instrumentation Engineering Department of Thapar University, Patiala is as authentic record of my own work carried under the supervision of Dr. Prasenjit Basak. It refers others researcher's work which are duly listed in the reference section. The matter contained in this dissertation has not been submitted, neither in part nor in full to any other degree to any other university or institute except as reported in text and references.

Place: Patiala
Date: 15/07/2016

(Rahul Tomar)
Roll No.: 801441021

It is certified that the above statement made by the student is correct to the best of my knowledge and belief.

Date: 15/07/16.

(Dr. Prasenjit Basak)
Assistant Professor
Electrical & Instrumentation Engineering Department
Thapar University, Patiala

Countersigned by:

(Dr. Ravinder Agarwal)
Head
Electrical & Instrumentation Engineering Department
Thapar University, Patiala

(Dr. S. S. Bhatia)
Dean (Academic Affairs)
Thapar University, Patiala

CERTIFICATE

Certified that the dissertation entitled, "**Comparison between Perturb & Observe Method and Incremental Conductance Method for Maximum Power Point Tracking of PV Module**", which is being submitted by **Rahul Tomar** in fulfillment of the requirements for the award of the **Master of Engineering in Power Systems**, to Thapar University, Patiala, is a bona-fide record of the candidate's own work carried out by him under my supervision and guidance. The matter contained in this dissertation has not been submitted, neither in part nor in full to any other university or institute for award of any degree.

Place: Patiala
Date: 15/07/16

(Dr. Prasenjit Basak)

ACKNOWLEDGMENT

I take the privilege to offer my deepest sense of gratitude to my supervisor Dr.Prasenjit Basak, for his constant motivation, support, and personal attention, which have proved to of immense help throughout my dissertation tenure. Under his guidance I successfully overcame many difficulties and learned a lot.

I am also thankful to Dr. Prakash Gopalan, Director of Thapar University, Patiala for providing the facilities for the completion of M.E. I express my deep sense of gratitude towards Dr Ravinder Agarwal, Head of the Department of Electrical & Instrumentation Engineering, Thapar University, Patiala for constantly encouraging each student to put their best foot forward in whatever field of work they take up, and Ms. Manbir Kaur, Associate Professor & PG Coordinator for her motivational approach.

I extend my gratitude to the researchers and scholars whose hours of toil have produced the papers that I have used in the dissertation. Finally, I take this opportunity to express my indebtedness to my family who are my source of optimism. Their wisdom and endearment motivate me to strive for excellence and keep my morale high, always.

Rahul Tomar
(801441021)

LIST OF ABBREVIATIONS

ABBREVIATIONS	CLARIFICATIONS
AC	Alternating Current
AM	Air Mass
ANN	Artificial Neural Network
ASTM	American Society for Testing and Materials
DC	Direct Current
GA	Genetic Algorithm
IDB	Interleaved Dual Boost
INC	Incremental Conductance
MPP	Maximum Power Point
MPPT	Maximum Power Point Tracking
P&O	Perturb and Observe
PI	Power Increment
PV	Photovoltaic
STC	Standard Test Condition

TABLE OF CONTENTS

TABLE OF CONTENTS(CONTINUED)

LIST OF TABLES

LIST OF FIGURES

NOMENCLATURE

SYMBOL	DESCRIPTION
I	Output current of PV module
I_{SC}	Short circuit current of PV module
I_{SCn}	Short circuit current of module in STC
I_{PV}	Generated current of PV module
I_{PVn}	Generated current of PV module in STC
I_O	Saturation current of diode
I_{MPP}	Output current of PV module at MPP
V_{MPP}	Output voltage of PV module at MPP
V_d	Diode voltage
V	Output voltage of PV module
V_{OC}	Open circuit voltage of PV module
L	Inductor
C	Capacitor
V_T	Thermal voltage of PV module
V_{Tn}	Thermal voltage of PV module in STC
k	Boltzmann constant
E_g	Bandgap energy
W	Width of depletion region of p-n junction
L_n	Number of electrons in p region of p-n junction
L_p	Number of holes in nh region of p-n junction
R_S	Series resistance of PV module
R_p	Parallel resistance of PV module
P_{MAXm}	Maximum output power of PV module
P_{MAXe}	Experimental maximum output power of PV module
N_S	Number of cell connected in series in module
K_i	Temperature coefficient of current
K_v	Temperature coefficient of voltage
V_r	Output Voltage of boost converter
V_{in}	Input voltage of boost converter
D	Duty ratio
ΔI_L	Current ripple through inductor

ΔV_C	Voltage ripple across capacitor
f_S	Switching frequency of MOSFET
I_r	Output current of boost converter
T	Actual temperature
T_n	Temperature corresponds to STC
G	Actual irradiance
G_n	Irradiance corresponds to STC
x	Direct optical path length through the Earth's atmosphere

ABSTRACT

Due to the mounting demand of electricity, inadequate reserve of fossil fuel and rising prices of conventional sources, photovoltaic (PV) energy becomes a promising substitute. It is a prevalent means of producing clean and renewable power and due to this reason, the demand of PV generation systems increases and there is a need to extract maximum power from them. So there is need of maximum power point tracking (MPPT) in a PV system. It is a technique that can operate solar PV systems in such a way that they produce maximum power that can be generated. MPPT tracking system works based on a tracking algorithm which is provided through a control system. In this dissertation, a comparison is made between perturb and observe MPPT method and incremental conductance MPPT method to make clear understanding about their behavior for tracking maximum power point (MPP) of PV module under constant and variable irradiation. For this purpose, a simple and accurate model of photovoltaic module is proposed and simulated. The output of the proposed module is connected with boost converter whose switching is controlled by the above mention MPPT techniques to ensure the satisfactory operation of PV module at MPP.

CHAPTER 1

INTRODUCTION

Energy is inevitable need for human. Use of fossil fuels in prolongation for meeting energy demand now lead to face multiple problems: depletion of fossil fuel reserve, rise in fuel cost, environmental concerns like global warming, change in weather patterns etc. These problems results in an unsustainable situation. Therefore there is an increasing need of renewable energy sources, as a result Photovoltaic (PV) generation is gaining significance, as a renewable source due to its various advantages like less running cost as there is no fuel required, no noise, less wear and tear due to absence of any rotating part, little maintenance etc. Solar energy is directly converted into electrical energy by photovoltaic cell (a semiconductor device). PV cell is a semiconductor diode which can convert light into direct current (DC). Some PV cells can even convert infrared and ultraviolet radiation into electricity. Although in 1839, Alexander-Edmond Becquerel discovered the photovoltaic effect, in a junction formed between electrode made of platinum and an electrolyte solution of silver chloride. However in 1939 first photovoltaic device is made by Russell ohl, by using a Silicon pn junction [1]. The basic unit of PV module is the PV cell. Cells are grouped to form module or arrays. PV cells can be made from several types of semiconductor material using different manufacturing procedure.

1.1 Working Principle of Solar Cell

Solar cell is basically a p-n junction as shown in Fig.1.1. The n region of a solar cell is made thin so that sunlight penetrates through it and it is heavily doped. The lightly doped p region shares most of the depletion layer. The penetration of sunlight depend on its wavelength and absorption of sunlight increases with decrease in wavelength, so shorter the wavelength higher the absorption coefficient and vice versa. The electron hole pair which is formed in the depletion region and due to its electric field, electrons remain in n-region and holes in p-region. When subjected to external load, surplus electrons of n region recombine with the excess holes of the p region as the circuit gets complete through the load. Some of the free electrons are also generated in the p region and holes are formed in n region. The shorter wavelengths of high absorption coefficient are absorbed in n region whereas longer wavelengths absorbed in broader p-region. Some of the electron hole pairs which are generated in these regions (electrons in p region and

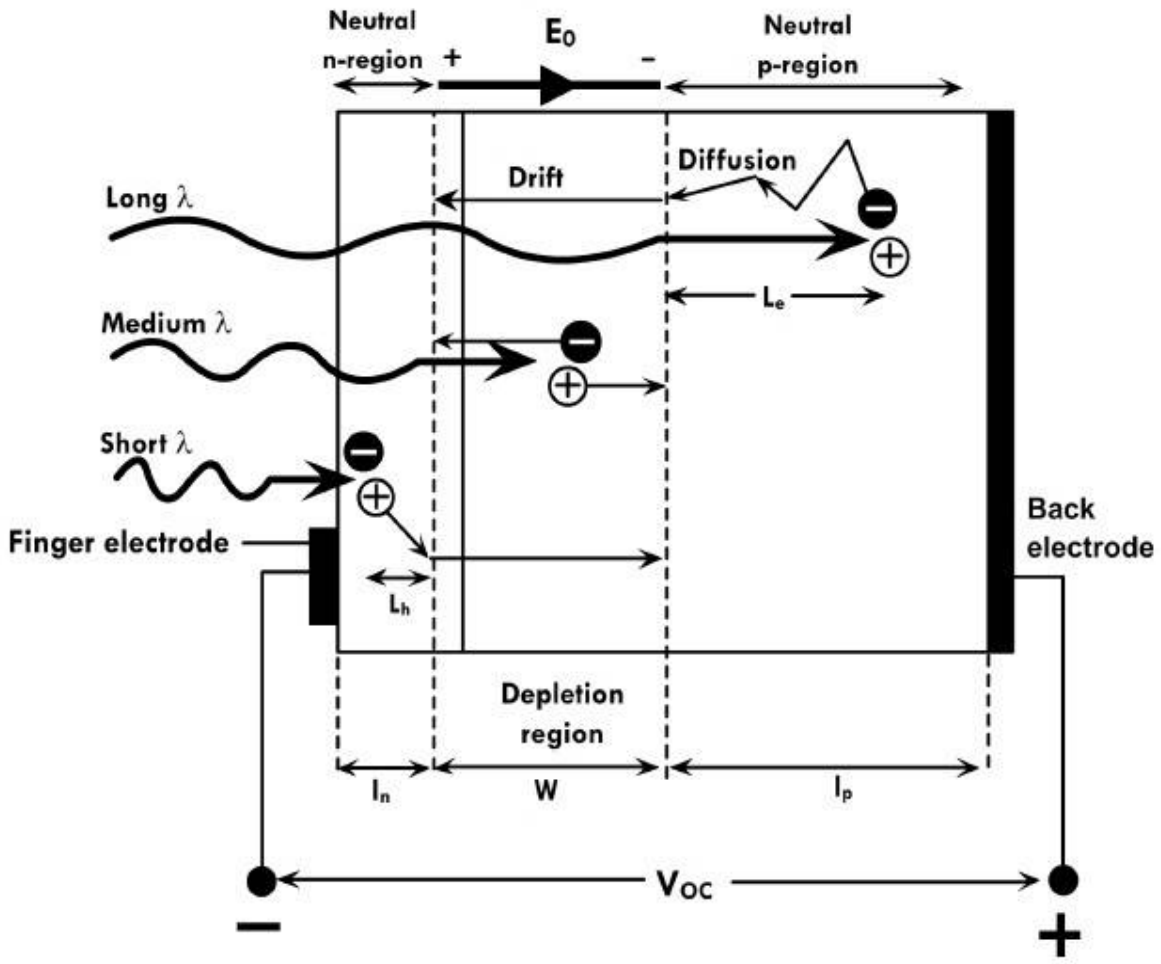

Figure 1.1 Operation of a p-n junction solar cell [1]

holes in n region) also have some contribution in the generated current. Typically, these electron hole pairs which are formed in minority carrier diffusion length, L_p notation used for holes in the n region and L_n notation for electron in p region. These minority carriers contribute to the current as they can also diffuse in depletion region. So, width of the area that has contribution in the current produced by module is $W + L_n + L_p$, as shown in Fig 1.2. The carriers are travel through the metal electrodes which are placed on either side of module. A small electrode is placed on the top in order to provide sufficient surface for sunlight to penetrate as shown in Fig 1.3. Consider a silicon made solar cell having a band gap (E_g) of 1.1 eV. So that when the incident radiation of wavelength above 1.1µm which possess the energy lower than that is required by electron to jump to conduction band so it is not absorbed by module and when the incident light wavelength is much smaller than 1.1µm so the absorption coefficient is huge and

the electron hole pair generated near surface are get trapped. So there is a certain optimum range of wavelengths where electron hole pairs can contribute photocurrent.

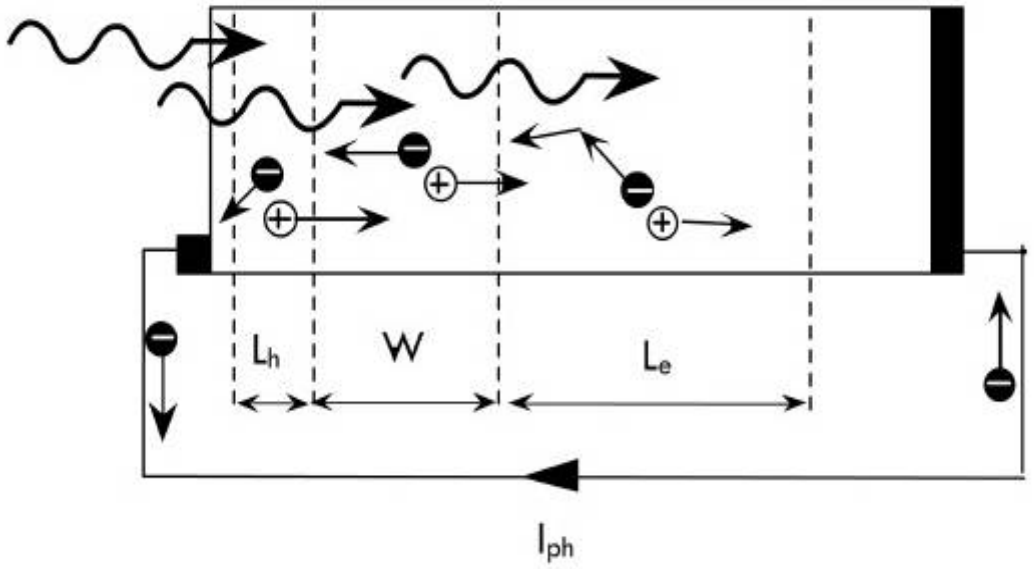

Figure 1.2 Photo generated carriers in solar cell [1]

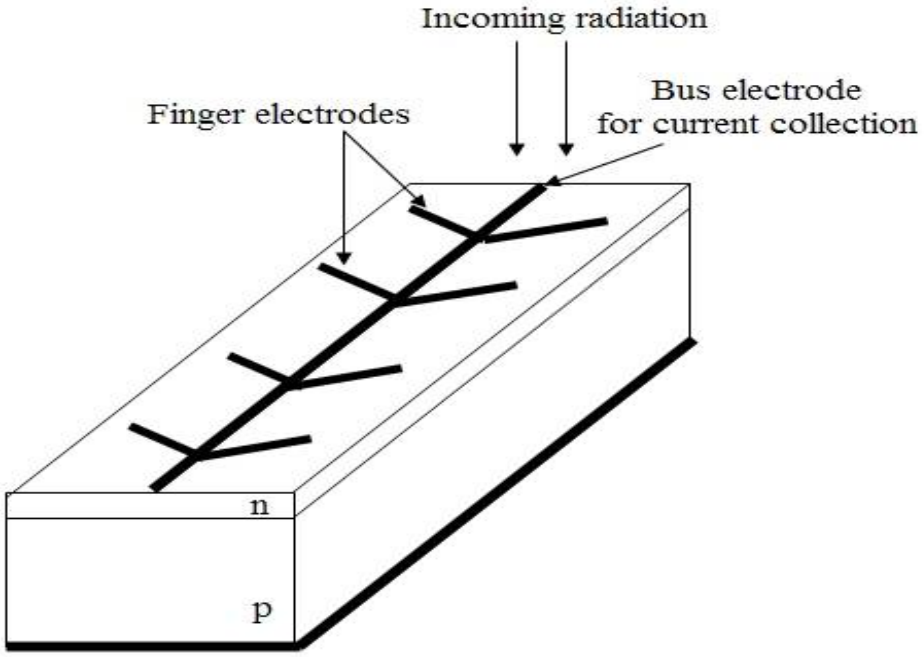

Figure 1.3 Finger electrodes on top of p-n junction solar cell [1]

1.2 Solar Radiation Spectral Distribution.

The PV device efficiency depends on the solar radiation spectral distribution .The Sun light radiation spectrum can be equated to the black body spectrum when it is at 5800K. All wavelengths of electromagnetic radiation are absorbed and emit by black body. This behavior of black body to distribute wavelengths is mathematically given by Planck's law, from which one can understand the relationship between interdependencies of frequency, temperature and black body spectral distribution [2]. From Fig1.4 one can observe black body spectral distribution and compared it with solar spectral distribution.

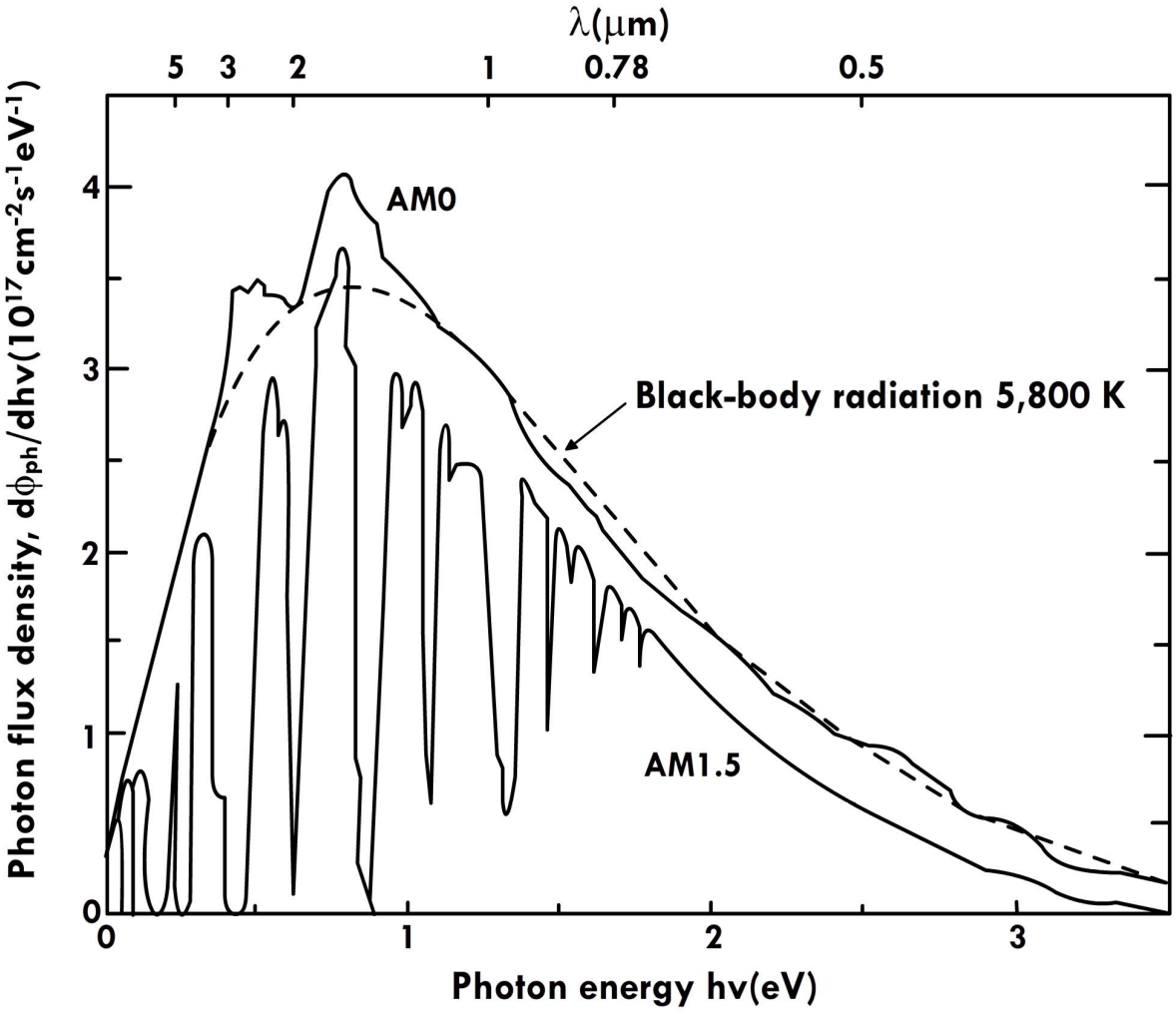

Figure 1.4 Solar spectral distribution [1]

To acknowledge the effect of solar radiation on PV module, study of various factor like changes in temperature of solar disc and how earth atmosphere mould solar radiation. The irradiation of

sun in the extraterrestrial space within earth and the sun is about 1.353 kW/m^2 but due to earth's atmosphere only 1kW/m^2 is the irradiation on earth's surface.

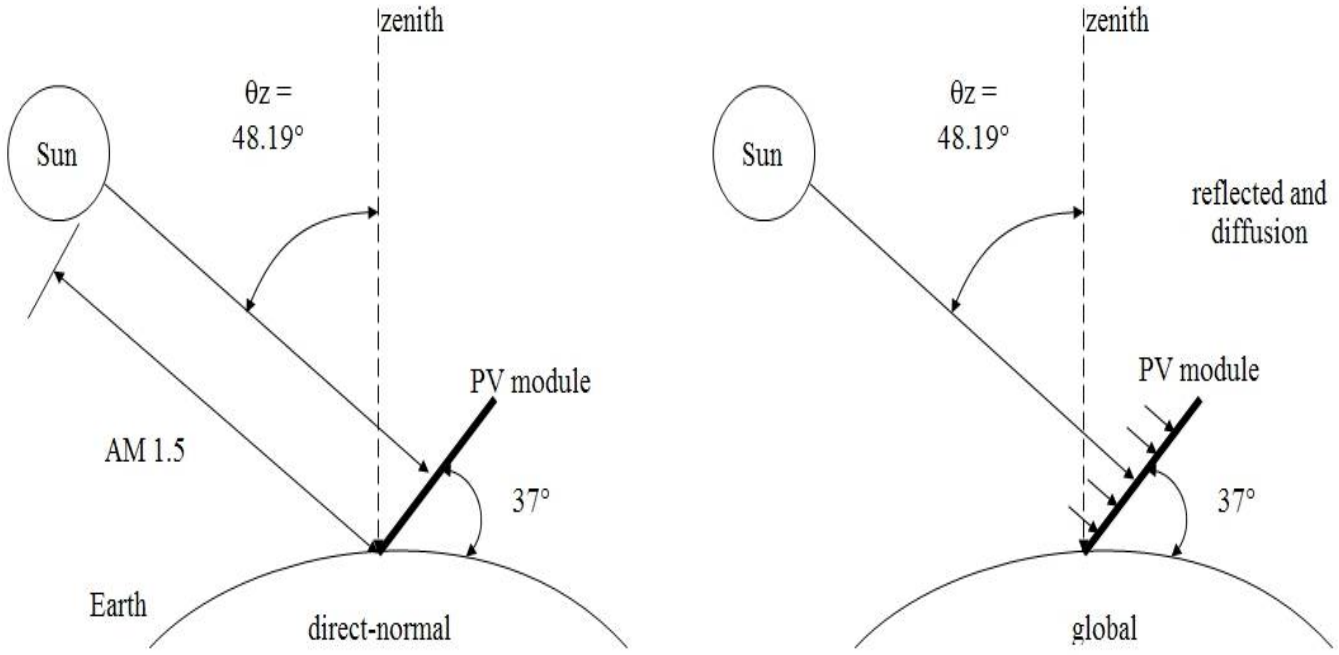

Figure 1.5 Diagram of AM1.5 pathway the direct normal and global incoming radiations on PV module facing sun and have 37ºC tilt position [29]

Evaluation of PV modules is generally accomplished with some reference standard spectral distribution. The American Society for Testing and Materials (ASTM) give the direct-normal spectral and global AM1.5 spectral. The direct-normal standard represents that part of incident solar radiation that is reaching perpendicular to sun facing surface. The global standard that is representing by AM1.5 is corresponding to the radiation spectrum of that of direct and diffuse radiations. The radiations which get influenced due to the earth's atmosphere are diffuse radiations. The ASTM defines AM1.5 for a PV device whose surface is tilted by an angle of 37ºC and it faces the Sun. The AM in AM1.5 imply 'air mass' that is mass of air within the surface and the Sun that affects intensity of solar radiation and its spectral distribution. The number (or coefficient) in AM1.5 represents the distance that sunlight travels through the atmosphere to reach PV module and the longer the distance, deviation and absorption of light increase. Due to these phenomena there is spectral distribution change in light that is received by the PV module. The path which has to travel by sun rays to reach the PV module is indicated by *x* of AM*x* and it is define as

$$x = \frac{1}{\cos\theta_Z} \tag{1.1}$$

Where θz is angle between incident solar radiation and the zenith, as shown in Fig 1.5. The solar radiation spectrum of standard AM1.5 is distribution correspond to θz = 48.19º

1.3 Literature Review

In order to utilize maximum energy from the PV module, tracking of maximum power point (MPP) is essential. There are many techniques in literature for maximum power point tracking (MPPT). These methods are differentiating from each other in various respects like convergence time, implementation complexity, degree of effectiveness, memory requirement, economic aspects etc. Teulings *et al.* [2], verified combination of digital hill climbing and bidirectional current control mode power cell control for MPPT as viable topology. But he was not considering changing weather conditions. Hiyama *et al.* [3], used proportional integral controller with neural network based MPPT technique to achieve MPP. Also check performance under changing weather conditions and conclude that tracking of MPP is quick with this method. But in this method neural network require time to learn the characteristics of PV module. Tsai Pan *et al.* [4], used linear current control for MPPT, as current at MPP posses linear relationship with irradiance and found current at MPP by sensing solar radiation and proportional control controller is used to track current at MPP. This technique is depend on type of PV array and there characteristics. Takashima *et al.* [5], computed current and voltage at MPP by sensing temperature and solar radiation intensity and then feedback control loop system forced PV array to operate at MPP. Drawback of this method is that the Computation of current and voltage at MPP on the basis of temperature and irradiance is difficult and different PV module have different value of current and voltage at MPP so this method depend on the parameter of the module. Veerachary *et al.* [6], used signal flow graph technique for interleaved dual boost (IDB) converter modeling and presented MPPT result for partial shading condition and changing irradiance and demonstrated that IDB is suitable for extracting maximum power from PV array in comparison to boost converter. The drawback of interleaved dual boost is that in this method switching losses is high. Fuzzy logic control boost converter based MPP tracking is reported [7]. This paper reveal that fuzzy control have improved MPPT performance with respect to conventional techniques. However, there is a drawback of this method as some of the parameters

are selected on a trial basis, which are chosen by designer to the best of his/her knowledge. This drawback can be overcome by fuzzy and neural network based MPPT technique proposed in [8]. But a neural network has to be trained for particular PV module for which it is going to be employ and also the neural network is to be trained at regular time intervals as characteristics of PV module vary with time. This drawback of neural network technique is overcome in [9], author demonstrated performance of PV system integrated with an inverter which provides the MPPT to the PV panels by switching frequency modulation scheme. He shows with 30-W laboratory prototype that this method can globally locate the MPP over wide irradiation. But this method implementation is complex and costly. ESRAM *et al.* [10], proposed ripple correlation control, which is easy in implementation and has dynamic response and have fast convergence speed. It is work on ripple produced in power which is produced when we connected PV panels with power converter (due to converter switching, ripple get produced in voltage and current which is reflected in power) . This method does not demand any prior data about PV panel characteristics. In principle, the ripple correlation control signals sampled at a very high rate and the continuous-time method is changed to discrete time .This requires sampling to be done at many times the switching frequency, therefore has limited practical merit. Femia *et al.*[11], shown that with the change in classical constant duty cycle in perturb and observe (P&O), by varying duty ratio such that it linearly reduces with increase in power extracted from the PV module, the stability and the power loss under steady state condition reduces but due to perturbation losses are still there. To solve these problems Liu *et al.* [12], proposed a modified incremental conductance (INC) MPPT method having varying step size which is tuned automatically with integral characteristic of PV array. This method has fast convergence as the step size is changes according to the position of operating point from MPP, step size increases when MPP is at a distant and step size reduces when MPP is nearby. The drawback of this method is that it has high Implementation complexity. Fortunato *et al.* [13], adopted jointly one cycle control and P&O approach for MPPT and track MPP under rapidly changing weather. But this method has fluctuations when operating point reached MPP. Gules *et al.* [14], used bidirectional two switch boost converter with P&O MPPT technique and increase in overall efficiency and reduction on the negative effect of power converter losses is achieved using parallel connection of MPPT system. Kwon *et al.* [15], proposed a three-phase PV system and MPPT is controlled by three-level boost converter. MPPT controller used hysteresis in power to

provide duty ratio control to three level boost converters for MPP tracking. The reduction in reverse recovery losses in diodes is observed using three-level boost converter and thus increase in the overall power efficiency. High implementation complexity, PV array dependency are drawbacks of this method. Chen *et al.* [16], used DC link capacitor droop control for MPPT, the method has easy implementation and has good convergence speed but this method doesn't have periodic tuning attribute due to which the operating point sometime get entrap in the local maxima. Ramaprabha *et al.* [17], presented Genetic Algorithm (GA) based offline trained Artificial Neural Network (ANN) to operate array at MPP. ANN has to be trained for different environmental condition and for a particular PV module. Verification of the method for different weather conditions was shown with reduced errors, which further get reduced by raising the training data for ANN. In this method periodic tuning is there but it requires lots of memory and implementation complexity is high. Hsieh *et al.* [18], proposed power-increment-aided INC (PI-INC) method for MPPT and presented that the two-phased tracking of PI-INC has fast and accurate MPPT in comparison to INC MPPT, on the basis of experiment performed under five different level of intensity of solar radiation on different tracking phenomena. Complexity of this method is high. Kollimalla *et al.* [19], projected two-stage variable perturbation size algorithm for MPPT and demonstrated with the help of experimental result that this method improved tracking speed under stable weather condition and has fast dynamic performance under varying operating condition. The demerit which is not removed by this method is steady-state oscillations around MPP. Paz *et al.* [20], proposed INC MPPT method with adaptive-step implementation which uses Lock- In Amplifier used for matching AC resistance of load to the DC resistance of PV panel, in order to achieve operation at MPP. The adaptive-step implementation expressed in this method reduces the INC algorithm to a simple discrete-time integral controller with a gain that adapts the step-size to produce fast and accurate tracking with minimal complexity, but not succeed in tracking MPP at changing weather condition.

1.4 Objective of the Dissertation

The objective of the work is to study P&O and INC MPPT techniques by simulating them using MATLAB/SIMULINK and to observe about their convergence speed to track MPP in steady state condition and under changing irradiation. For the implementation of this technique on a PV module, simulation of TATA make TP240 PV module is done. The datasheet of TP240 is taken

from [21] and the unknown parameter that is the value of resistances is calculated under standard test condition (STC) using iterative method in which curve fitting is done using Newton-Raphson method. The output of the PV module is given to boost converter whose switching is varied by MPPT technique to ensure the operation of module at MPP.

1.5 Dissertation Organization

The dissertation titled as –"Comparison between perturb & observe method and incremental conductance method for maximum power point tracking of PV module" has been organized in six chapters. **Chapter 1** deals with working principle of solar cell, solar radiation spectral distribution**,** literature review, objective of the dissertation. **Chapter 2** represents the evolution of practical equivalent circuit for PV cell, theory of PV module. **Chapter 3** contains equations essential for modeling of PV module and algorithm to found the value of unknown parameter of PV module and modeling aspects. **Chapter 4** contains algorithm of P&O and INC MPPT techniques. **Chapter 5** contains selection parameter for boost converter and result and discussion on the behavior of MPPT techniques under changing irradiation. **Chapter 6** contains conclusion and future scope.

CHAPTER 2

EQUIVALENT CIRCUIT OF PV CELL

2.1 Ideal Equivalent Circuit

In literature there are various equivalent circuit used for simulation of PV module. Like in [22] two diode model is used to interpret recombination effect of charge carriers. In [23] three-diode model is employed to quantitatively analyze output operation of multi-crystalline silicon solar cells with high leakage current through its periphery and its electrical properties. Single diode model is explained below. As this model have well balance between simplicity and accuracy [24]. In single diode model, some have neglected series resistance R_S [25] [26] as it has very small value and some neglected parallel resistance R_P as it possess high value [27][28]. Equivalent circuit of a simple PV cell consists of a diode in parallel with current source .The current source turn in current which is directly proportional to sun irradiation .There are two consideration of interest for PV cell equivalent circuit and they are :

- The current which flows when terminals are shorted (short circuit current, I_{SC})
- The voltage across terminals when the terminals are open (open circuit voltage ,V_{OC})

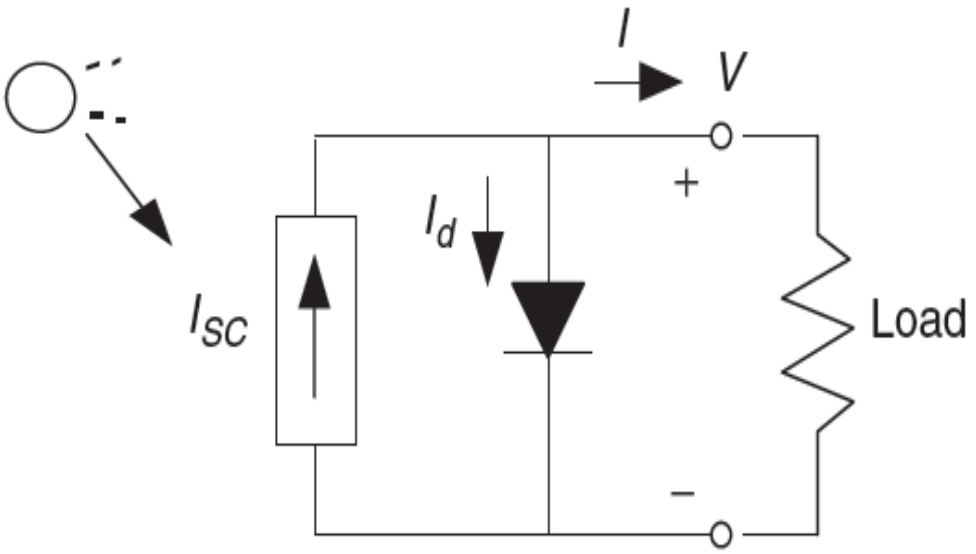

Figure 2.1 Equivalent circuit of ideal PV cell.

When terminals of the PV cell (equivalent circuit) are shorted then no current pass through the diode as voltage across diode is zero (V_d=0), so current generated by the current source

completely flow from the shorted terminal leads and that current must be equal to short circuit current (I_{SC}). Output Current from equivalent circuit of PV cell is

$$I = I_{SC} - I_d \tag{2.1}$$

Where: I_{SC} is light generated current in equivalent ideal circuit.

I_d is current through diode

It is known from Shockley diode equation that the voltage –current relation of p-n junction is:

$$I_d = I_O(e^{\frac{qV_d}{kT}} - 1) \tag{2.2}$$

Where: q is charge of the electrons (1.602×10^{-19} C)

k is Boltzmann constant (1.3806×10^{-23} J/K)

T is junction temperature (K)

V_d is diode terminal voltage

I_O is diode saturation current

Substitute equation (2.2) into (2.1)

$$I = I_{SC} - I_O(e^{\frac{qV}{kT}} - 1) \tag{2.3}$$

Where V is ideal PV cell output voltage

When PV cell terminals are left open, that is current is zero (I=0) and open circuit voltage is given by

$$V_{OC} = \frac{kT}{q}\ln(\frac{I_{SC}}{I_O} + 1) \tag{2.4}$$

And at 25ºC (298.15 K), equation (2.3) and (2.4) become

$$I = I_{SC} - I_O(e^{38.9V} - 1) \tag{2.5}$$

$$V_{OC} = 0.0257\ln(\frac{I_{SC}}{I_O} + 1) \tag{2.6}$$

Current generated from the solar panel is in directly proportional to solar irradiation and in above equation (2.5) and (2.6) short circuit current is therefore is in directly proportion with solar irradiation. So we can plot PV current voltage curves for varying solar irradiation (Figure 2.2) and it is visible from *I-V* curve that short circuit current value becomes half when the irradiation

decrease to half (linear relation follows) but there is not much effect on the value of open circuit voltage.

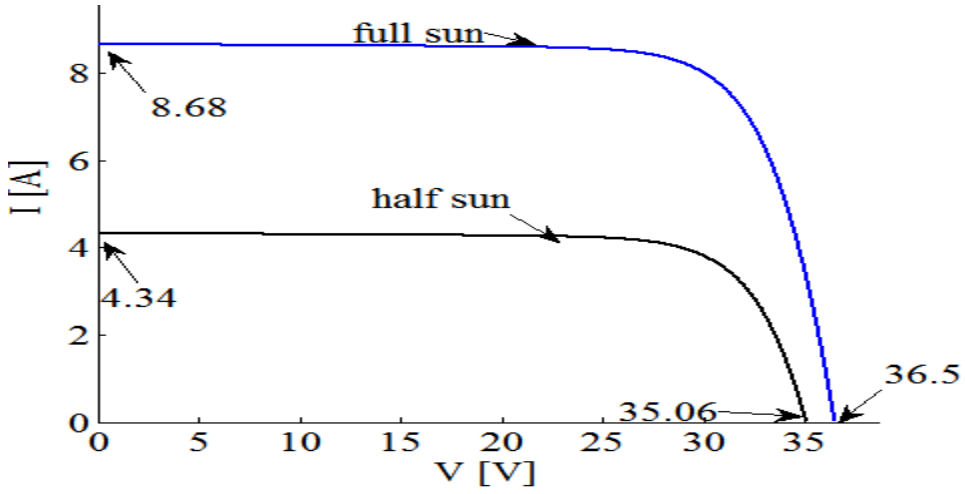

Figure 2.2 PV module *I-V* characteristics on full sun and half sun

2.2 A More Accurate Equivalent Circuit

There are requirement of more complex PV equivalent circuit than shown in figure 2.1. The need of another equivalent circuit can be explain with the help of a problem. Consider that there is shading on one of the cell (as shown in figure 2.3)

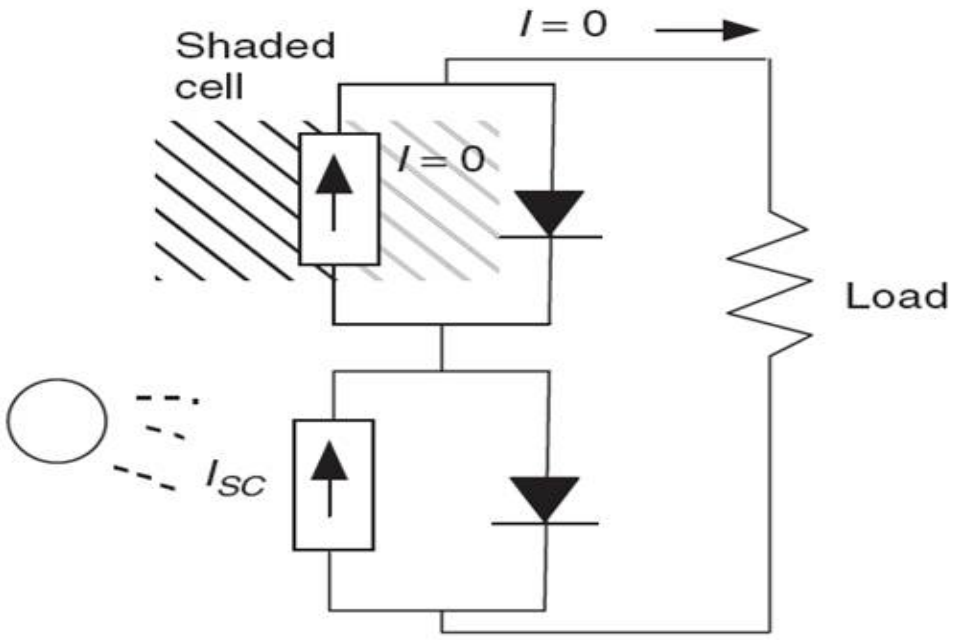

Figure 2.3 Effect of partial shading

So it produces zero current and the diode which is in parallel is also reverse biased so the cell not allows any current to pass through it. So, this mean with above equivalent circuit no current will pass in such condition. For this reason there is a need of more complex model. So, the parallel resistance R_P is contributed in the circuit as a solution to above problem. The current sources now supply current to diode, resistance connected in parallel and the load.

The equation of output or load current is written below.

$$I = (I_{SC} - I_d) - \frac{V}{R_P} \tag{2.7}$$

$$I = (I_{SC} - I_d) - \frac{V}{R_P} \tag{2.8}$$

From this equation we can say that at any given voltage, now the load current decreased by V/R_P (as shown in figure 2.4)

The equivalent circuit is even get better when we consider a series resistance along with parallel resistance. Before we come to that model, we discuss model shown in fig. in which ideal PV cell equivalent circuit modified to have series resistance, R_S .this additional resistance R_S include contact resistance between PV cell and conductor leads associated with them and the resistance of PV cell's semiconductor material.

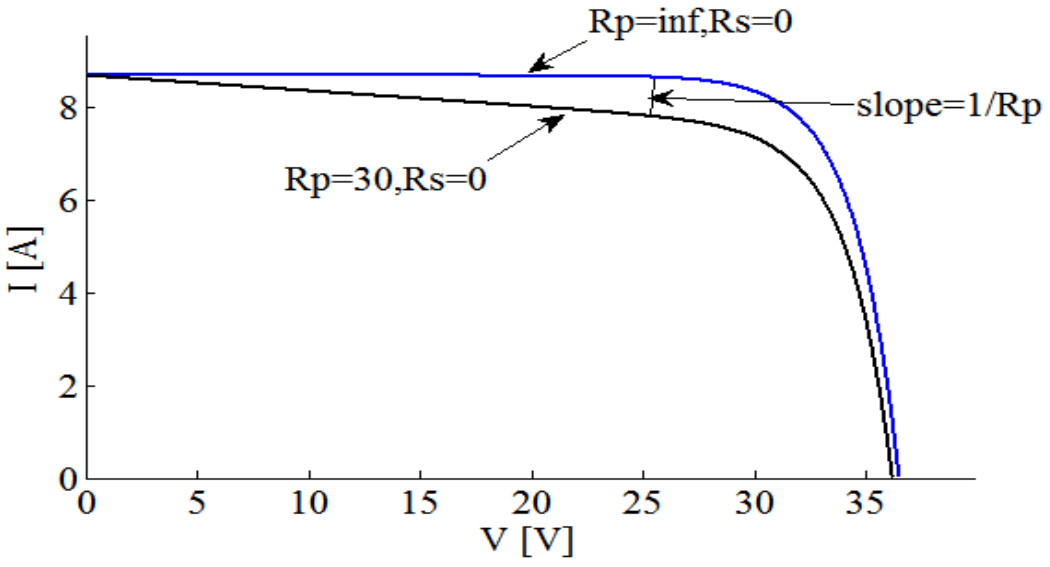

Figure 2.4 Effect of R_P addition on I-V curve

To analyze the effect of adding R_S, take equation (2.1) of simple PV cell equivalent circuit

$$I = I_{SC} - I_d = I_{SC} - I_O\left(e^{\frac{qV_d}{kT}} - 1\right) \tag{2.9}$$

And due to adding R_S, voltage across diode changes

$$V_d = V + IR_S \tag{2.10}$$

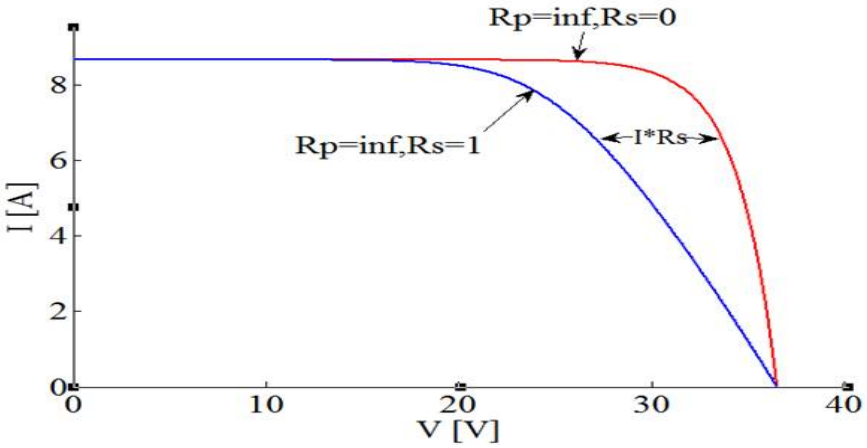

Figure 2.5 Effect of R_S *I-V* characteristics curve

So changing the value of V_d in equation,

$$I = I_{SC} - I_O\left(\mathrm{e}^{\frac{qV+IR_S}{kT}} - 1\right) \tag{2.11}$$

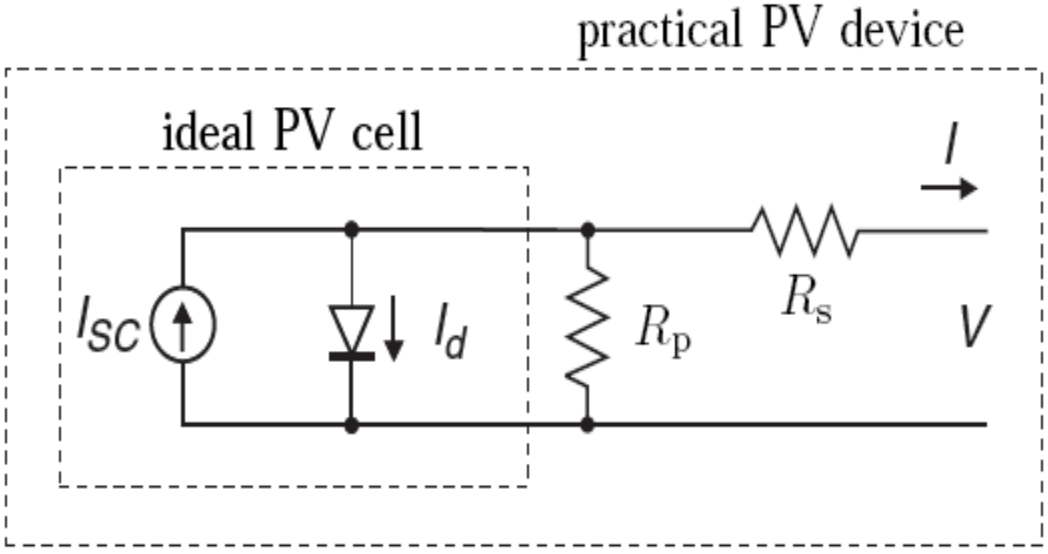

Figure 2.6 Practical single diode model of PV cell

Finally, we came to generalized equivalent model where we consider both R_S and R_P .So the current and voltage equation for this generalized circuit:

$$I = I_{SC} - I_O \left\{ e^{\left[\frac{q(V+IR_S)}{kT} \right]} - 1 \right\} - \left(\frac{V + IR_S}{R_P} \right) \quad (2.12)$$

2.3 PV Module

The output voltage which an individual cell can produce is about 0.5 V, which is very less. For getting more voltage which can be used, combination of solar cells is needed. A PV module is a bundled, linked assembly of solar cells connected in series or in parallel. Solar cells connected in series to increase module output voltage and in parallel for increase in current. Module is building block of PV system. Rating of module is done by its DC output power tested under standard test conditions (STC) (25ºC temperature and irradiation of 1000W/m²). PV module is designated either by maximum power which they can provide or by the number of cell they posses. A typical module has 36 cells. Now a days modules having large number of cells are quite common for example KC200GT has 54 PV cells, TP240 has 60 PV cells etc. There are four production technologies for PV Modules which are Single crystalline, Polycrystalline or Multi-crystalline, String ribbon and Amorphous or Thin Film. Single crystalline is oldest, expensive and most efficient technique among all. Polycrystalline or Multi-crystalline is economic with slightly lower efficiency in comparison to single crystalline process. String ribbon has low manufacturing cost and efficiency compared to above two methods. Amorphous method is cheapest method and has low efficiency among all. Two or more PV module assembled to form a PV panel.

2.4 Maximum Power Point (MPP)

Maximum power from the PV module is extracted when the voltage across the load is equal to voltage at maximum power point and load is such that it extracts current equal to current at maximum power point, that is the maximum power at Standard Test Condition (STC). The knee point shown in I-V curve (figure 2.7) represent maximum power point. The operational output power of the PV module depends on its efficiency which is depending upon module technology used at the time of manufacture. The MPP point for our TP240 which is (V_{MPP},I_{MPP}) is (29.7, 8.1) as shown in figure 2.7

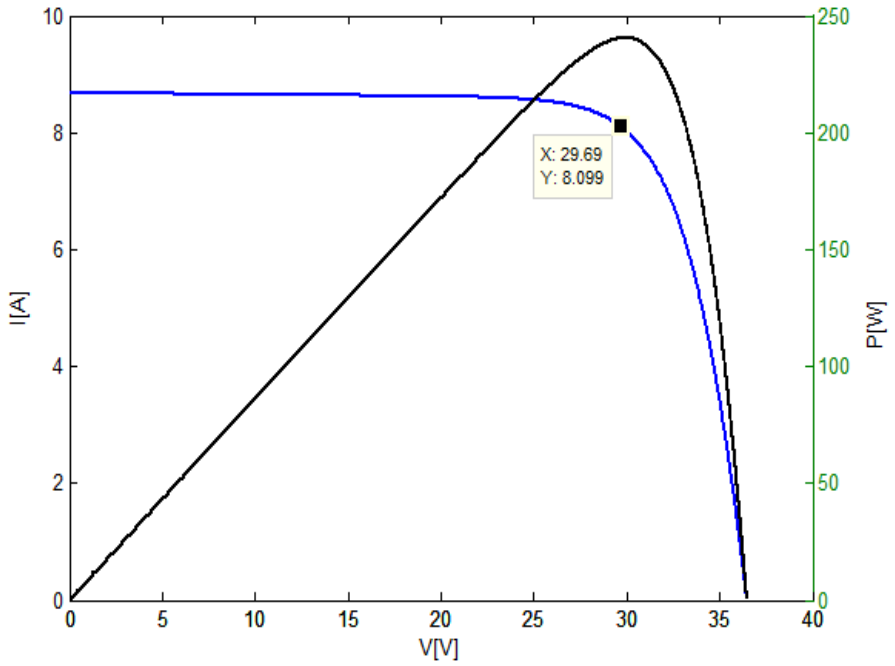

Figure 2.7 Overlap *I-V* and *P-V* characteristics curve describing significance of MPP

2.5 Fill Factor

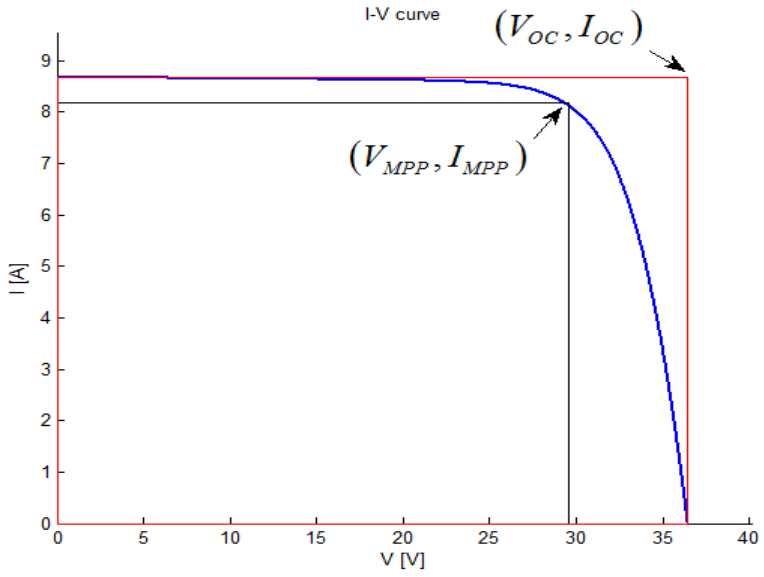

Figure 2.8 Fill factor is the ratio of power at MPP to the area formed by rectangle with sides V_{OC} and I_{SC}.

The fill factor is defined as the ratio of the maximum rectangle which can fit inside the *I-V* curve to the rectangle circumscribing the curve as shown in figure 2.8.The fill factor is directly linked

with the electrical output power. Fill factor of a PV module is given by the manufacturer under standard test condition (STC). Fill factor significance is that it will measure the performance of the PV module, greater the fill factor more is the output power and greater the efficiency.

$$FF = \frac{V_{MPP} I_{MPP}}{V_{OC} I_{OC}} \tag{2.13}$$

$$EFFICIENCY(\eta) = \frac{P_{MAXm}}{P_{IN}} = \frac{FF \times V_{OC} \times I_{SC}}{P_{IN}} \tag{2.14}$$

CHAPTER 3

Modeling of PV Module Using Two Diode Model

3.1 Modeling of PV Module:

The equation which defines the *I-V* characteristic of PV module is obtained in chapter 2, is written for module having N_S number of cells connected in series.

$$I = I_{SC} - \left\{ I_O \exp\left[\frac{q(V + IR_S)}{kTN_S} \right] - 1 \right\} - \left(\frac{V + IR_S}{R_P} \right) \tag{3.1}$$

All PV module manufacturer mention three remarkable points regarding module in their datasheets which is nominal open-circuit voltage (V_{OCn}) when the module is open circuited in STC , the nominal short-circuit current (I_{SCn}) when the output terminal of module is shorted under STC, the voltage and current at MPP when the module is delivering maximum power. Temperature coefficient of voltage (i.e. represent by K_V) and of current (represent by K_I) and experimentally check max peak output power of PV module (represent by P_{MAXe}) and the number of cells (represent by N_S) in a module, these information are also presented in datasheet of a PV module. In practical PV module series resistance *Rs* have more impact when device is operating in region where it acts as a voltage source and parallel resistance R_P have more impact in current source region (as shown in Fig 3.1).

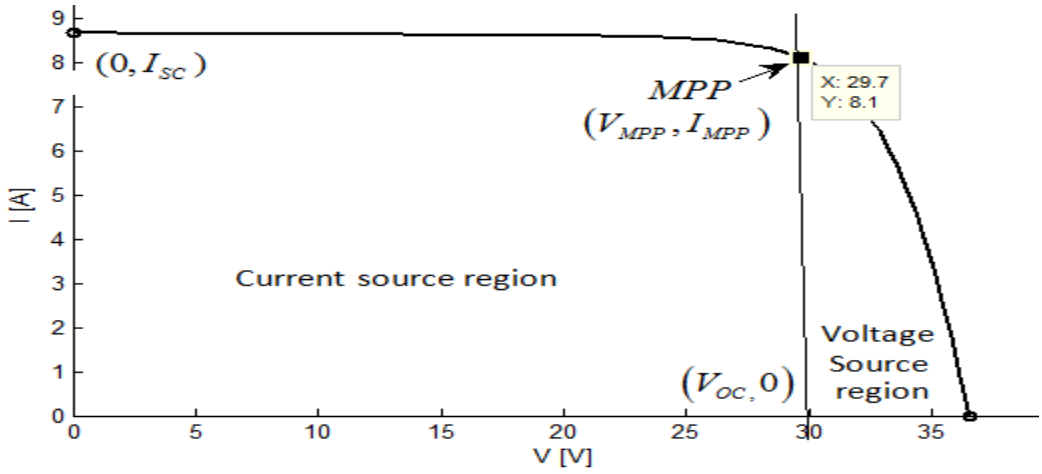

Figure 3.1 I-V characteristic curve of practical PV module

For modeling of PV module I_{SC} is take approximately equal to I_{PV} (Where I_{PV} is current generated by PV module) because generally value of the series resistance is low and of parallel

resistance is high. The current generated in module due to sunlight is linearly depends on the solar irradiation and also have temperature influence given by following equation

$$I_{PV} = (\mathrm{I}_{PVn} + K_I \Delta_T)\frac{G}{G_n} \tag{3.2}$$

Where: I_{PVn} is the current generated due to sunlight at STC (usually 25 ◦C and 1000W/m^2), $\Delta T = T - T_n$ (where T is actual temperature and T_n is temperature at STC)

G is actual irradiation and G_n is irradiance at STC.

The influence of temperature on diode saturation current [29] is expressed as

$$I_O = I_{On}\left(\frac{T_n}{T}\right)^3 \exp\left[\frac{qE_g}{ak}\left(\frac{1}{T_n} - \frac{1}{T}\right)\right] \tag{3.4}$$

Where E_g is band gap energy of semiconductor material and I_{On} is nominal saturation current

$$I_{On} = \frac{I_{SCn}}{\exp\left(\frac{V_{OCn}}{aV_{Tn}}\right)} \tag{3.5}$$

Where V_{Tn} is thermal voltage at nominal temperature of N_S series connected cells and $V_{Tn}=N_S kT/q$.

Now we consider the effect of temperature coefficient of current (K_I) and voltage (K_V) on saturation current so that open circuit voltages match with the experimental data for a wide range.

$$I_O = \frac{I_{SCn} + K_I \Delta_T}{\exp(\frac{V_{OCn} + K_V \Delta_T}{aV_T}) - 1} \tag{3.6}$$

3.2 Adjustment Made in Module

Two parameter R_S and R_P are left unknown in eq. (3.1). In order to adjust *Rs* and *Rp*, such that maximum power that can be generated by module mentioned in datasheet should be equal to experimental power generated and both *I-V* and *P-V* curve should be match with experimental data. As we know the open circuit voltage and short circuit current, so the range of voltage and current is known we have to find such value of R_S and R_P so that all the points with mainly three remarkable point (which are open circuit voltage V_{OCn} ,MPP , short circuit current I_{OCn}) must

match. The relation between R_S and R_P constituted by equating P_{MAXm} = P_{MAXe} and solving resulting equation for R_S

$$P_{MAXm} = V_{MPP}\left\{I_{PV} - I_O\left[\exp\left(\frac{q}{kT}\frac{V_{MPP}+R_S I_{MPP}}{aN_S}\right)-1\right]-\frac{V_{MPP}+R_S I_{MPP}}{R_P}\right\} = P_{MAXe} \tag{3.7}$$

$$R_P = V_{MPP}\frac{\left(V_{MPP}+I_{MPP}R_S\right)}{\left\{V_{MPP}I_{PV} - V_{MPP}I_O\exp\left[\frac{\left(V_{MPP}+I_{MPP}R_S\right)}{N_S a}\frac{q}{kT}\right]+V_{MPP}I_O - P_{MAXe}\right\}} \tag{3.8}$$

From eq. (3.8) we get value of R_P for any value of R_S such that the *I-V* curve touch the experimental maximum point (V_{MPP},I_{MPP}) .

Before starting the iterative procedure to get the value of R_S and R_P initial guesses are good so that convergence rate increases. As R_S is practically have small value so initially we take it zero, Initial value of R_P is

$$R_{P,MIN} = \frac{V_{MPP}}{I_{SCn} - I_{MPP}} - \frac{V_{OCn} - V_{MPP}}{I_{MPP}} \tag{3.9}$$

This equation represents the slope of line between point (*0*, I_{SCn}) and (V_{MPP}, I_{MPP}). This is a good initial guess for R_P.

For modeling purpose TP240 data is used from [23]:

Table 4.1 Parameters of the TP240 PV module at STC as provided in its datasheet

I_{MPP}	8.10
V_{MPP}	29.7
$P_{MAX,e}$	240
I_{SC}	8.68
V_{OC}	36.5
K_V	-0.2931
K_I	0.0442
N_S	60

Algorithm: For identify the value of R_S and R_P.

Step1: Input the data of module TP240 which are available in datasheet.

Step 2: Input value of constants (like Boltzmann constant, value of electron charge etc) and those parameter whose value is not dependent on variable or unknown parameters

Step 3: Define the tolerance value of power, step increment in value of R_S and number of step for which we want to plot I-V characteristic and input initial guess of R_S and R_P and set error value to infinity

Step 4: Start the while loop till the absolute value of error (P_{MAXe}-P_{MAXm}) is less than tolerance

Step 5: Calculate the value of I_{PVn} and I_{PV} as these values depend on R_S and R_P so with increment in R_S and R_P these value is updated with each iteration. Increments the values of R_S from 0 to some step increment value calculate value of R_P with the value of R_S using equation update the value of R_P.

Step 6: Solve the *I-V* equation for several (*V,I*) pairs (set in step 3) and for incremented value of R_S and R_P. This is done using Newton-Raphson method

Step 7: Plot the *I-V* and *P-V* curve. Update error value (P_{MAXe}-P_{MAXm}) end the loop and until the absolute of error value is not less than tolerance the loop is repeated (from step 4).

Step 8: Display the value of all parameter.

Table 4.2 Parameters of the adjusted model of the TP240 at STC

I_{MPP}	8.10
V_{MPP}	29.7
P_{MAXe}	240.57
I_{SC}	8.68
V_{OC}	36.5
$I_{O,n}$	1.06797e-07
I_{PV}	8.683255
A	1.3
R_P	357.837641
R_S	0.132

3.3 Simulation of PV Module

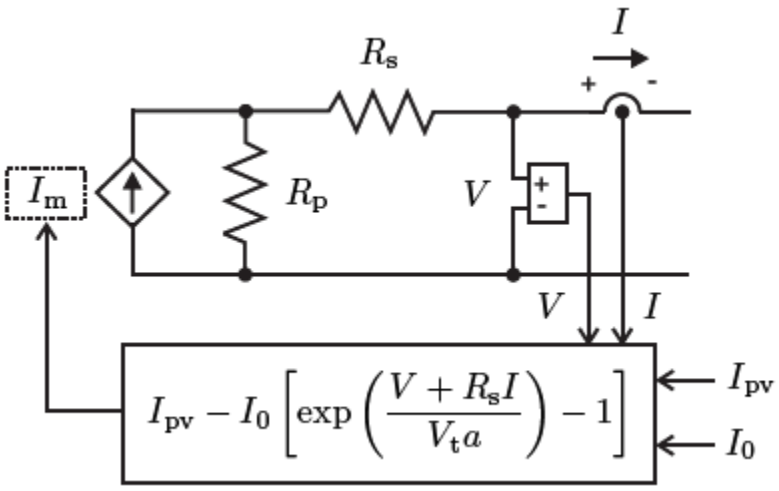

Figure 3.2 PV module circuit for simulation [29]

Now using these parameter and the equations above one can simulate this module in MATLAB/SIMULINK. The photovoltaic module is simulated with an equivalent circuit model shown in Figure 3.2, in which a circuit model having one current source (I_m) and two resistors (R_P and R_S). The value of temperature and irradiance is provided by externally. The value of the current I_m is I_{PV}-I_d .

$$I_m = I_{PV} - I_O \left[\exp\left(\frac{(V + IR_S)q}{akN_S T} \right) - 1 \right] \tag{3.10}$$

Where I_{PV} and I_O is calculated using eq. (3.1) and (3.6)

The voltage and current are given using voltage and current sensing. The value of I_{PV} , I_O and I_m is calculated from in MATLAB/SIMULINK using simple product, divide, addition and subtraction block and PV module output voltage and current(when load is applied) is obtain at output which is given to boost converter.

CHAPTER 4

SIMULATION OF MPPT TECHNIQUES

4.1 P&O

In the P&O method, one voltage sensor is required to sense the PV module voltage and therefore the implementation cost is less. The algorithm requires one perturbation on the duty ratio of the boost converter and other perturbation on the terminal voltage of the boost converter. When we perturb the duty ratio of the boost converter the terminal voltage of boost converter gets modified accordingly. In this method, we check the last perturbation sign and the sign of the last increase in the power to determine the next perturbation. This is get more clarified from Fig. 4.1 that when we move towards MPP with increase in voltage power also increase after MPP with further increase in voltage there is decrease in the power. The perturbation is to be continued in same direction till the power being incremented when the power starts decreasing then the direction of perturbation should be reverse. By keeping these facts in mind an algorithm is designed as shown by the flowchart in fig.4.2, and the loop is continued till MPP is achieved. As in this method we vary only reference voltage therefore implementation is easy. However this is not the best suitable method, as it cannot track MPP when there is sudden change in irradiation. An alternative approach to overcome this drawback and to track MPP with some more accuracy is shown in incremental conductance method

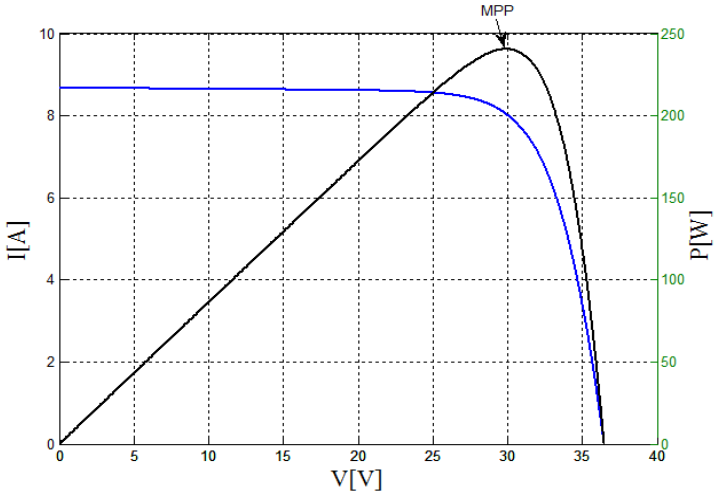

Figure 4.1 PV module characteristics curve

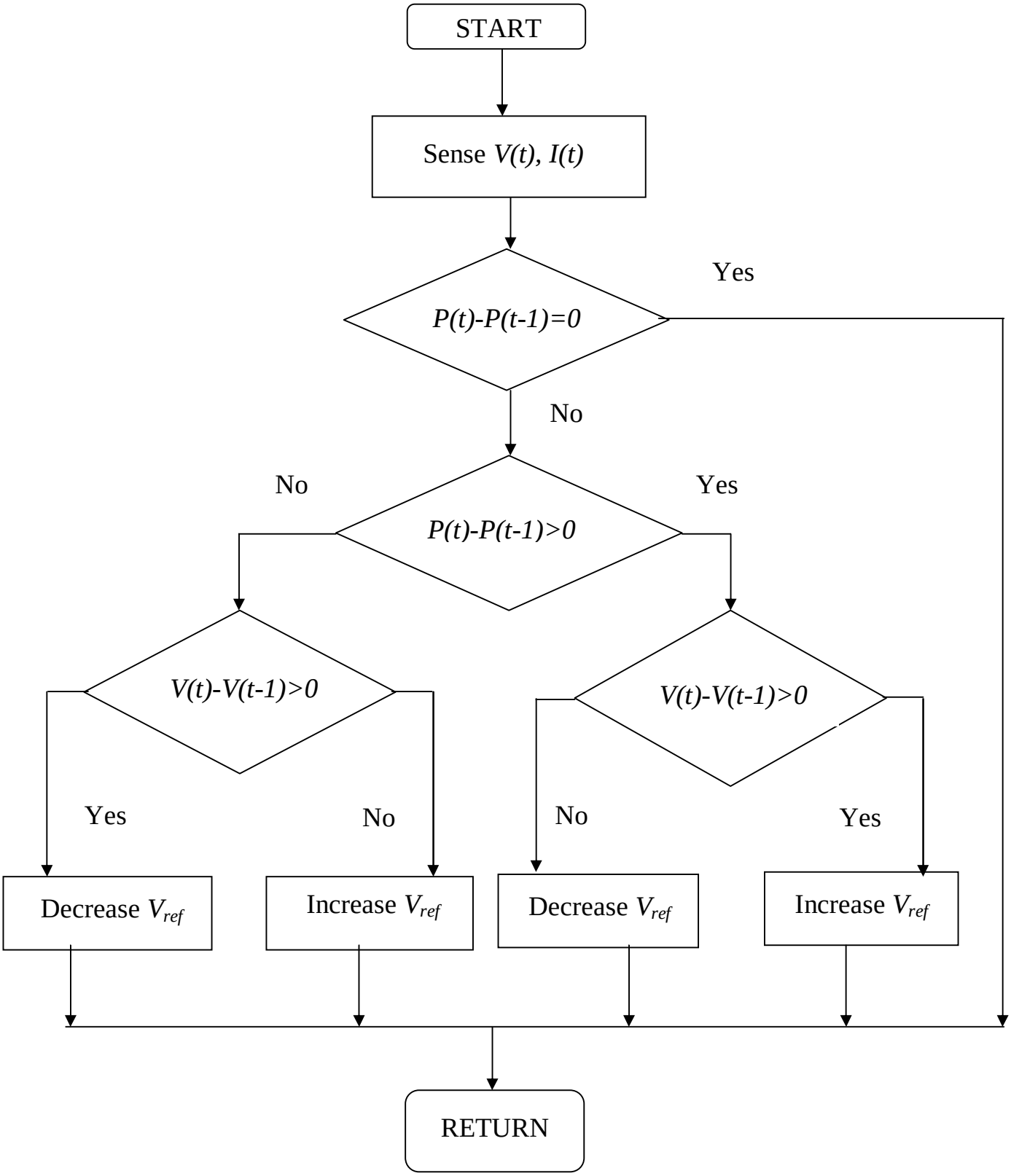

Figure 4.2 P&O algorithm

4.2 INC

The incremental conductance is based on information that the slope of PV module is zero at MPP, has increasing slope on left side of MPP and decreasing slope on Right side. The mathematical equations are as given below.

$$\frac{dP}{dV} = 0 \text{ (At MPP)} \tag{4.1}$$

$$\frac{dP}{dV} > 0 \text{ (At left of MPP)} \tag{4.2}$$

$$\frac{dP}{dV} < 0 \text{ (At right of MPP)} \tag{4.3}$$

Since

$$\frac{dP}{dV} = \frac{d(IV)}{d(V)} = I + V\frac{dI}{dV} \cong I + V\frac{\Delta I}{\Delta V} \tag{4.4}$$

So the above equation become

$$\frac{\Delta I}{\Delta V} = -\frac{I}{V} \text{ (At MPP)} \tag{4.5}$$

$$\frac{\Delta I}{\Delta V} > -\frac{I}{V} \text{ (At left of MPP)} \tag{4.6}$$

$$\frac{\Delta I}{\Delta V} < -\frac{I}{V} \text{ (At right of MPP)} \tag{4.7}$$

The ratio of current and terminal voltage ($\Delta I/\Delta V$) is incremental conductance of the output terminal and (I/V) is instantaneous value of conductance. To operate solar PV module at MPP the value of incremental conductance plus instantaneous conductance is equal to zero and at MPP V_{ref} is set to V_{MPP} . Once MPP attain, the PV module operation is kept at this point. When the alteration in ΔI is noted, means there is change in atmospheric condition , so there is change in MPP and in order to track new MPP V_{ref} is changed accordingly (incremented or decremented as shown in algorithm). The speed of this method to track MPP depends on increment size, but if increment size make small, oscillation at steady state decrease, but it take time to reach MPP and if the increment size is large, this will result in high amplitude oscillation at MPP. So increment size selected such that an optimal balance is maintained between speed at oscillation.

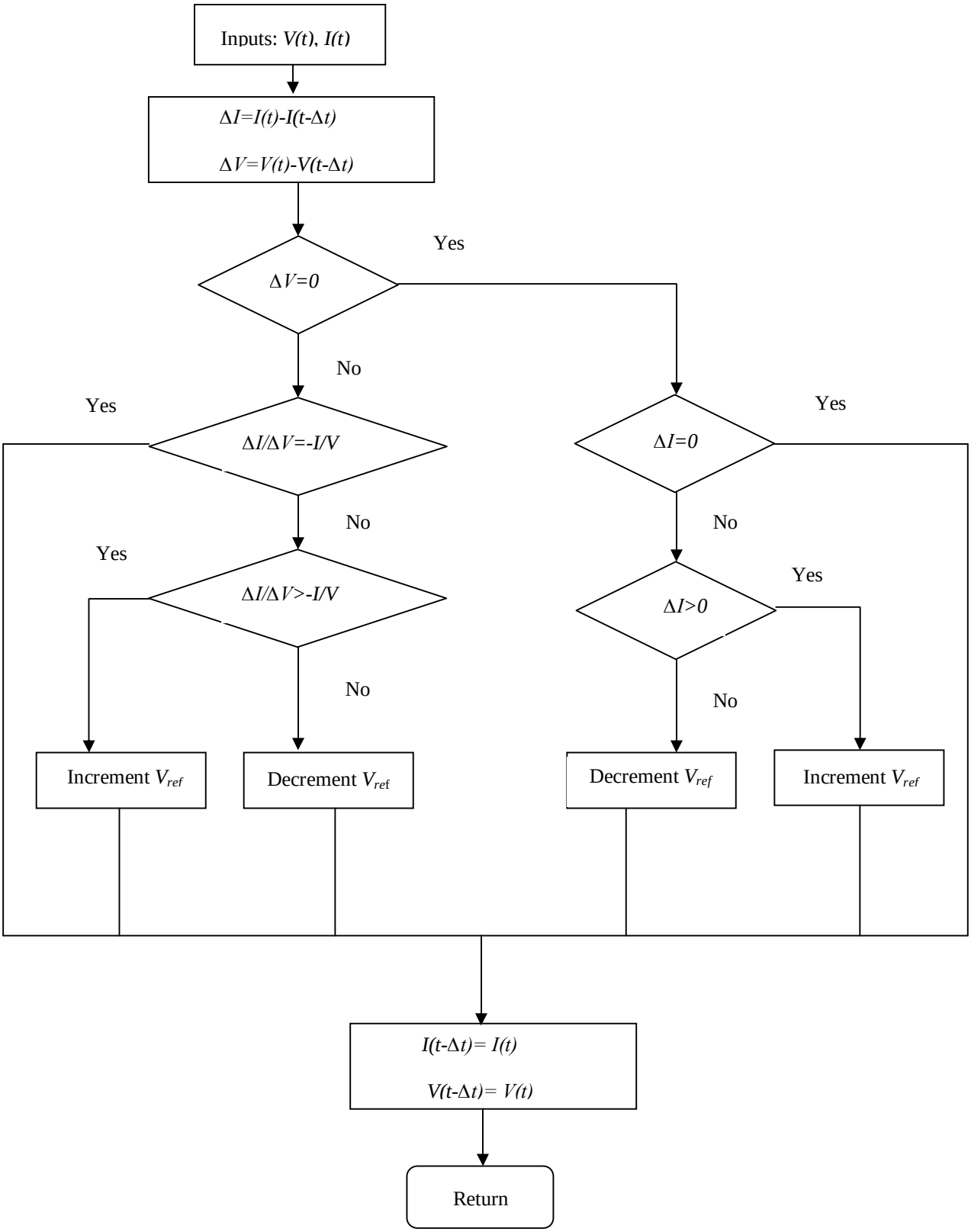
Inputs: V(t), I(t)
ΔI=I(t)-I(t-Δt)
ΔV=V(t)-V(t-Δt)
ΔV=0
Yes
No
ΔI/ΔV=-I/V
Yes
No
ΔI/ΔV>-I/V
Yes
No
Increment Vref
Decrement Vref
ΔI=0
Yes
No
ΔI>0
Yes
No
Decrement Vref
Increment Vref
I(t-Δt)= I(t)
V(t-Δt)= V(t)
Return

CHAPTER 5

RESULTS AND DISCUSSION

5.1 Selection of Boost Converter Parameters

PV module is connected to output resistive load through DC-DC boost converter. For switching in boost converter MOSFET is used. The duty ratio of boost converter is controlled by pulse generated via MPPT technique. These pulses are generated by comparing a carrier wave to control signal. Elements, inductor (L) and capacitor (C) ,values are selected through following equations

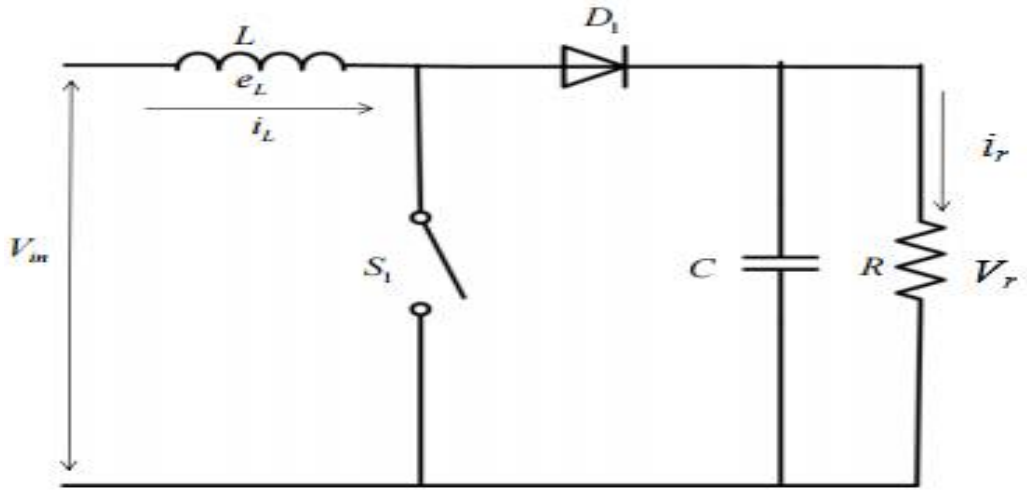

Figure 5.1 DC-DC boost converter

$$L = \frac{V_{in} D}{\Delta I_L f_S} \tag{5.1}$$

$$C = \frac{I_r D}{\Delta V_C f_S} \tag{5.2}$$

Where: V_{in} is boost converter input voltage

D is duty ratio

ΔI_L is ripple current through inductor

f_S is switching frequency

ΔV is voltage ripple across capacitance.

For PV module (TP-240) maximum output voltage is 29.7 V DC, this is input voltage for boost converter. If boost converter output voltage of 150 V is selected. So the duty ratio of boost converter is calculated using following equation:

$$V_r = \frac{V_{in}}{(1-D)} \tag{5.3}$$

$$150 = \frac{29.7}{(1-D)} \tag{5.4}$$

$$D = 0.802 \tag{5.5}$$

For output resistance of 100 Ω, output current is 1.5 A. Switching frequency is selected 20 kHz such that the ripple current through inductor should not more than 40% of that of load current. Ripple current of 10% (0.15 A) is selected. Output voltage ripple should be within 2%. Ripple of 1% (1.5 V) for output voltage is selected. Value of inductor and capacitor is

$$L = \frac{29.7 \times 0.802}{0.15 \times 20000} = 7.9398mH \tag{5.6}$$

$$C = \frac{1.5 \times 0.802}{1.5 \times 20000} = 40.1\mu F \tag{5.7}$$

For simulation these values are selected.

5.2 Irradiation Effect on TP240

PV module output power is depend upon incident irradiation. As we know that the short circuit current (*Isc*) is in direct proportion to irradiation and also with the increase of irradiation the maximum value of open circuit voltage (V_{OC}) increases exponentially. So with the increase in irradiation there is considerable increase in I_{SC} in comparison to V_{OC}. The effect of irradiation on TP240 is observed, the *I-V* characteristics under changing irradiance and at constant temperature (25ºC) is plot as shown in Figure 5.2 and the effect of irradiation on *P-V* curve at constant at temperature (25ºC) is shown in Figure 5.3

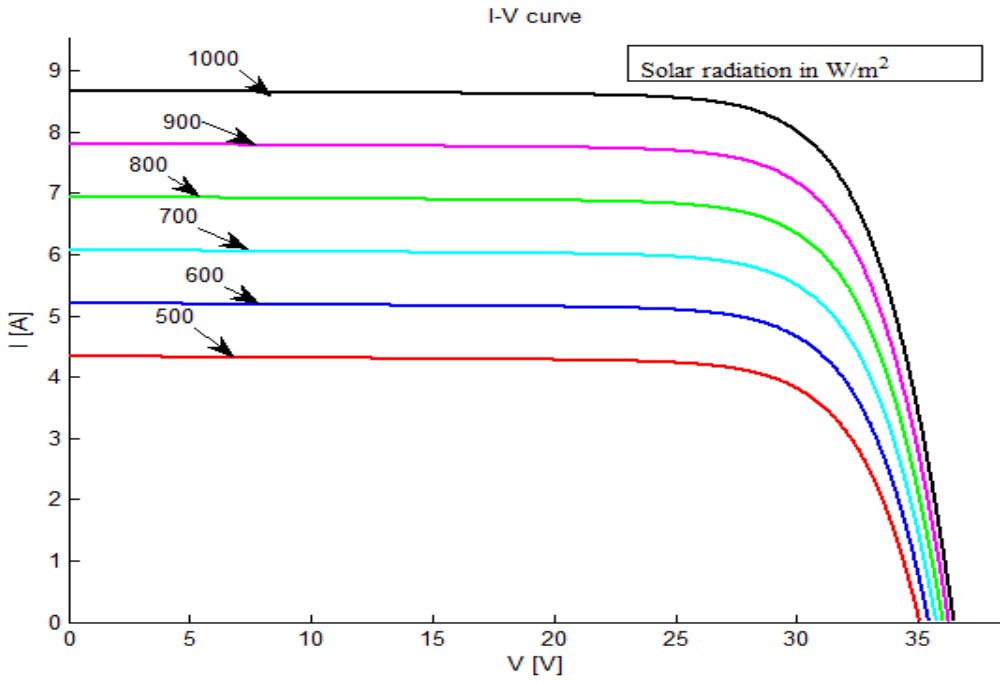

Figure 5.2 Effect of irradiation on *I-V* characteristics of TP240 at 25ºC

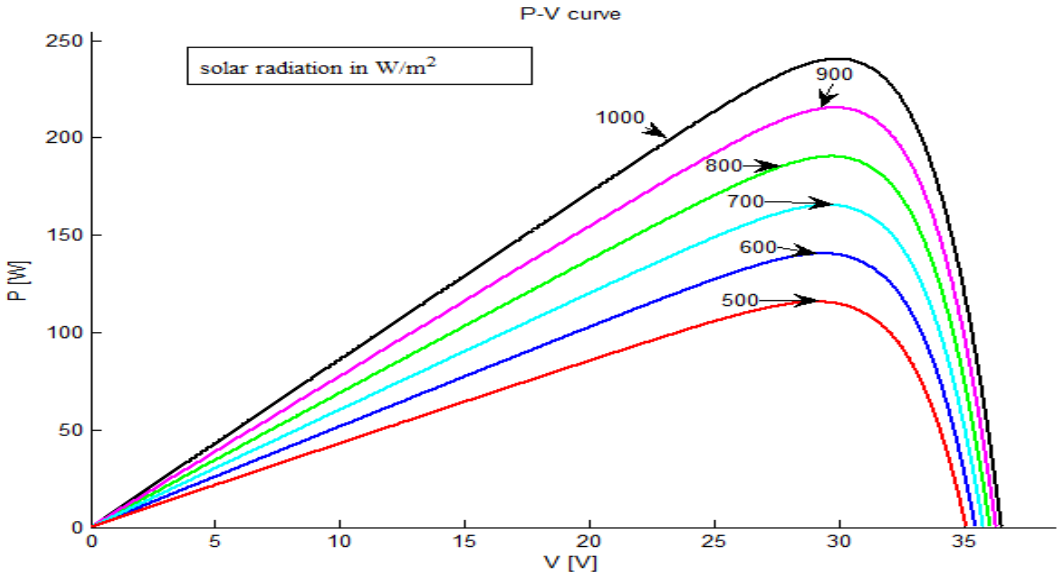

Figure 5.3 Effect of irradiation on *P-V* characteristics of TP240 at 25ºC

5.3 Temperature Effect on TP240

Module temperature is changes with the change in ambient temperature. Short circuit current (I_{SC}) increases marginally with the increase of PV module temperature more than the nominal temperature, that is 25^{o}C (298.15K) .But there is a considerable impact of PV module

temperature on the open circuit voltage (V_{OC}) when module temperature increases above nominal temperature open circuit voltage reduces. Increase in current due to module temperature increase is much lower than decrease in voltage so that the overall output power is reduced. The effect of temperature on TP240 is observed, the *I-V* characteristics under varying temperature and at constant irradiance (1000W/m^2) is plot as shown in Figure 5.4 and the effect of temperature on *P-V* curve at constant at irradiance (1000W/m^2) is shown in Figure 5.5.

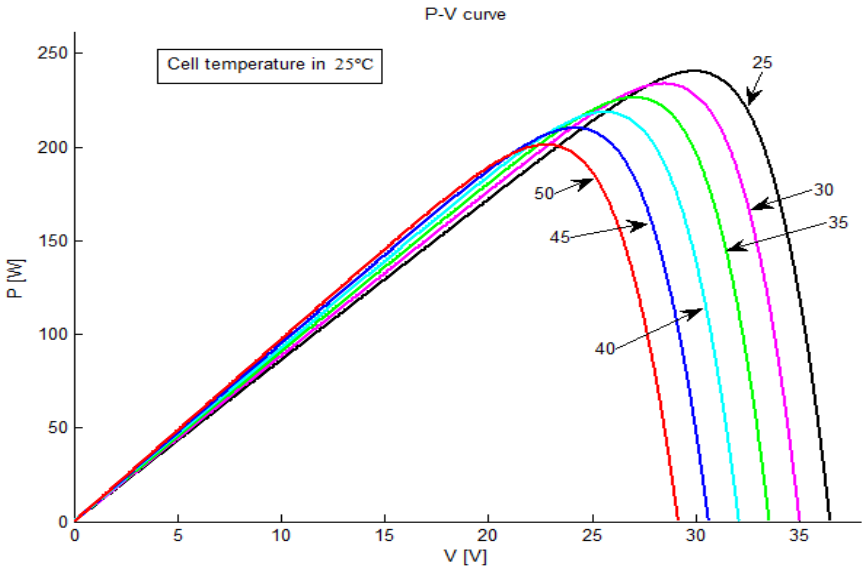

Figure 5.4 Effect of temperature on *P-V* curve of TP240 under constant irradiation (1000W/m^2)

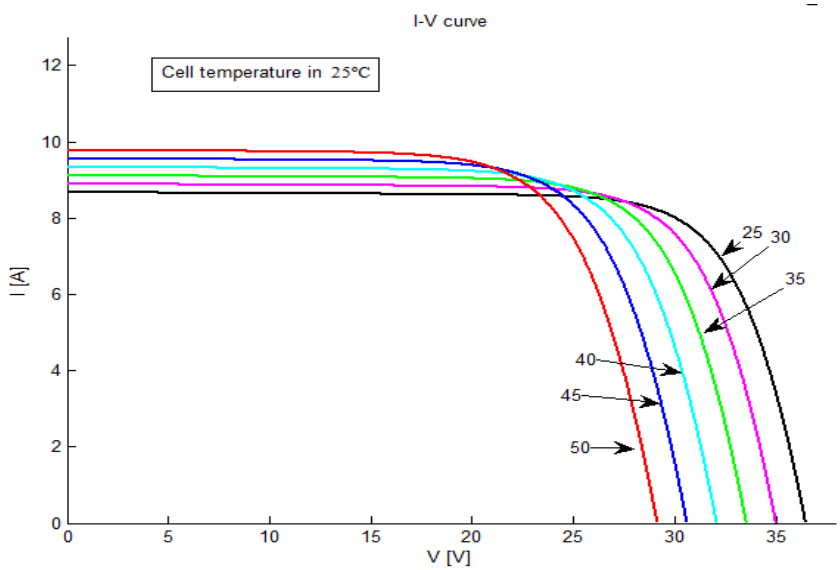

Figure 5.5 Effect of temperature on *I-V* characteristics of TP240 under constant irradiation (1000W/m^2)

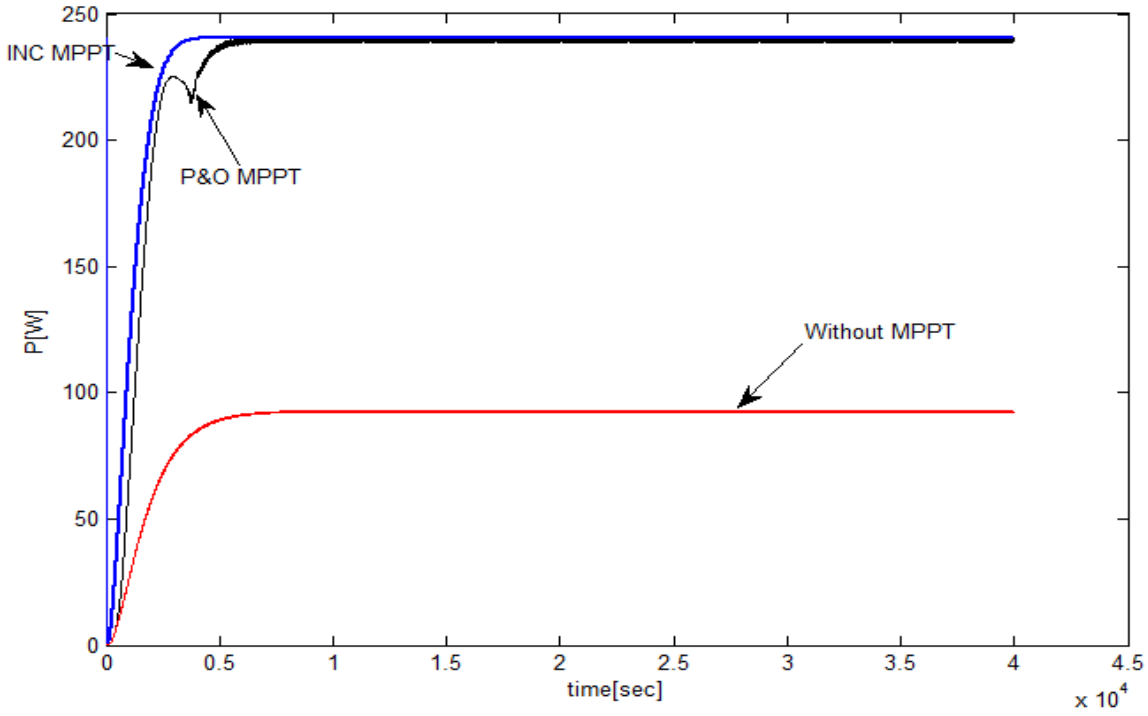

Figure 5.6 **Comparison at constant irradiance (1000W/m^2)**

5.4 Comparison between P&O and INC under constant irradiance

The output power variation with the MPPT technique used is shown in Fig5.6, black line represent output power corresponds to P&O MPPT technique and blue line represent output power when INC MPPT technique is used and red line represent output power without using any MPPT technique in this pulse generator provide pulse (at same frequency as used in P&O and INC MPPT techniques) to the boost converter.

5.5 Comparison between P&O and INC under varying irradiance

The comparison of INC and P&O in changes insolation is shown in Fig 5.7. The first irradiation level is 1000W/m² so the tracking of MPP occurs as stated above. When the irradiation level reduces to 600W/m² it is observed that the INC method reaches the steady state quickly as the steepness of output power (corresponds to INC) is greater which is shown in Fig.5.8. The same behavior is observed when irradiation further decrease to 400 W/m². It is clearly visible that INC technique achieves steady state condition quickly in comparison to P&O method and there is more fluctuation in output power resulted using P&O in comparison to INC.

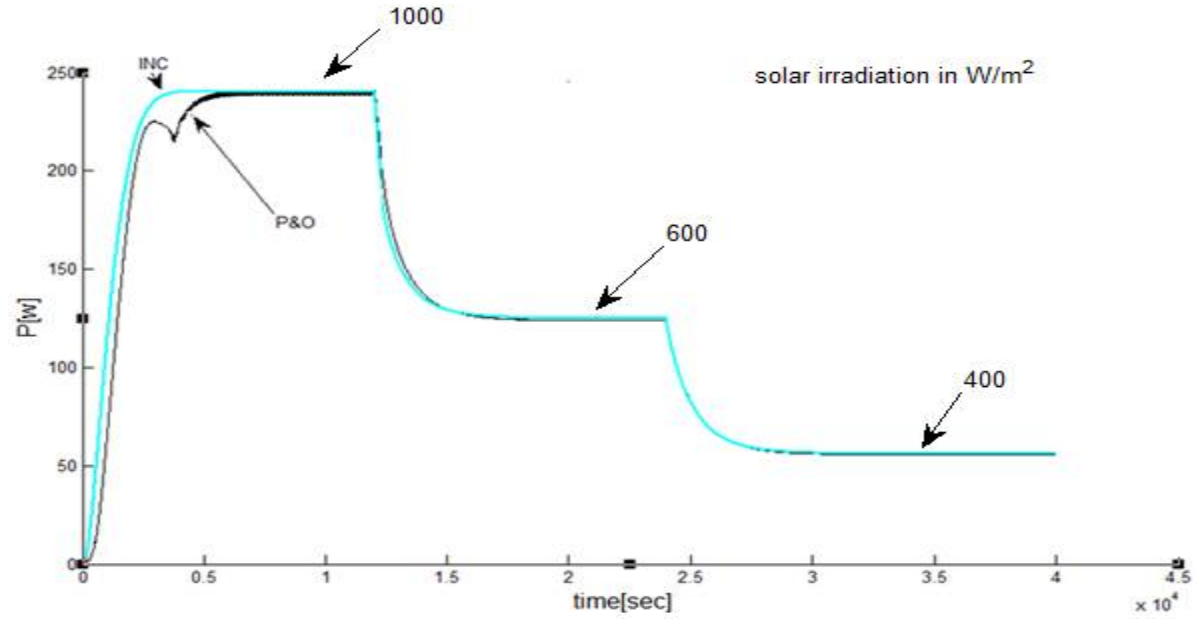

Figure 5.7 Comparison of P&O and INC method under changing irradiance at constant temperature (25C)

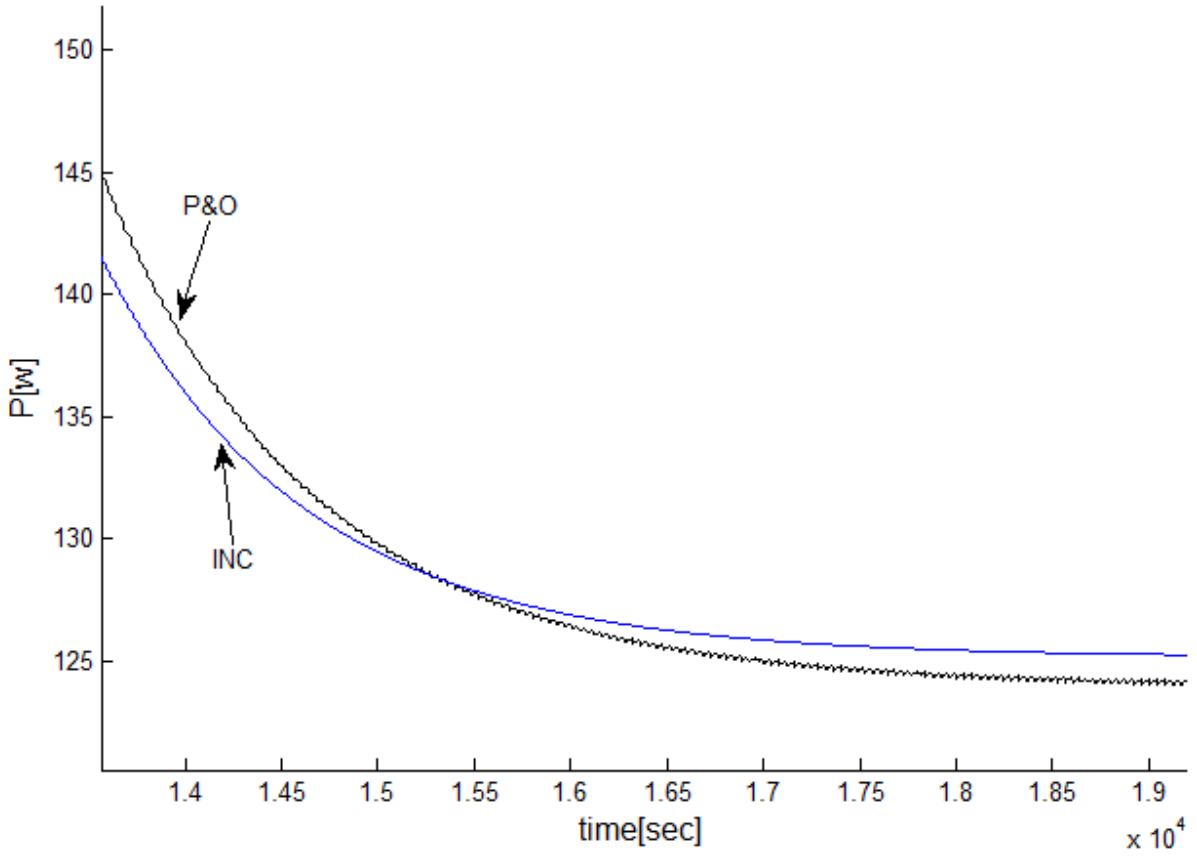

Figure 5.8 P&O and INC convergence speed for MPP tracking

CHAPTER 6

CONCLUSIONS AND FUTURE SCOPE

The MPPT technique must be implemented with every PV system. As MPPT technique enhances the overall efficiency of PV system. Model for comparison of two classical MPPT techniques is established using single diode model of PV cell. P&O is most admired method among all other method because of its simplicity and low implementing cost. But this method has disadvantage like fluctuations in steady state due to perturbation, unable to track MPP with fast change in irradiation. To overcome this disadvantage, perturbation step size should decrease but fluctuations in steady state are not permanently removed and due to these fluctuations some power loss occurs at steady state. So in order to make sure tracking of MPP under abrupt changes in irradiance, INC MPPT technique is implemented and experimentally determines fast response of INC method in comparison to P&O.

Under partial shaded conditions, the P&O and INC methods not work suitably as they get lock in local maxima because these methods cannot identify global maxima point as these are working on perturbation and the direction of perturbation is identify on the basis of change in power or change in voltage. So recently developed artificial intelligence technique can be used to determine global maxima in case of partial shading condition. Once the global maxima is identified then these methods can use to reach MPP.

Bibliography

[1] "Lecture 19: solar cell". [Online]. Available: http://nptel.ac.in/courses/113106062/Lec19.pdf. Accessed: 15-05-2016

[2] W. J. A. Teulings, J. C. Marpinard, A. Capel, and D. O'Sullivan, "A new maximum power point tracking system," in *Power Electronics Specialists Conference, 1993. PESC '93 Record., 24th Annual IEEE*, Jun 1993, pp. 833–838.

[3] T. Hiyama, S. Kouzuma, T. Imakubo, and T. H. Ortmeyer, "Evaluation of neural network based real time maximum power tracking controller for pv system," *IEEE Transactions on Energy Conversion*, vol. 10, no. 3, pp. 543–548, Sep 1995.

[4] C.-T. Pan, J.-Y. Chen, C.-P. Chu, and Y.-S. Huang, "A fast maximum power point tracker for photovoltaic power systems," in *Industrial Electronics Society, 1999. IECON '99 Proceedings. The 25th Annual Conference of the IEEE*, vol. 1, 1999, pp. 390–393 vol.1.

[5] T. Takashima, T. Tanaka, M. Amano, and Y. Ando, "Maximum output control of photovoltaic (pv) array," in *Energy Conversion Engineering Conference and Exhibit, 2000. (IECEC) 35th Intersociety*, vol. 1, 2000, pp. 380–383 vol.1.

[6] M. Veerachary, T. Senjyu, and K. Uezato, "Maximum power point tracking control of idb converter supplied pv system," *IEE Proceedings - Electric Power Applications*, vol. 148, no. 6, pp. 494–502, Nov 2001

[7] ——, "Feedforward maximum power point tracking of pv systems using fuzzy controller," *IEEE Transactions on Aerospace and Electronic Systems*, vol. 38, no. 3, pp. 969–981, Jul 2002.

[8] ——, "Neural-network-based maximum-power-point tracking of coupled-inductor interleaved-boost-converter-supplied pv system using fuzzy controller," *IEEE Transactions on Industrial Electronics*, vol. 50, no. 4, pp. 749–758, Aug 2003.

[9] B. M. T. Ho and H. S.-H. Chung, "An integrated inverter with maximum power tracking for grid-connected pv systems," *IEEE Transactions on Power Electronics*, vol. 20, no. 4, pp. 953–962, July 2005.

[10] T. Esram, J. W. Kimball, P. T. Krein, P. L. Chapman, and P. Midya, “Dynamic maximum power point tracking of photovoltaic arrays using ripple correlation control,” *IEEE Transactions on Power Electronics*, vol. 21, no. 5, pp. 1282–1291, Sept 2006.

[11] N. Femia, D. Granozio, G. Petrone, G. Spagnuolo, and M. Vitelli, “Predictive adaptive mppt perturb and observe method,” *IEEE Transactions on Aerospace and Electronic Systems*, vol. 43, no. 3, pp. 934–950, July 2007.

[12] F. Liu, S. Duan, F. Liu, B. Liu, and Y. Kang, “A variable step size inc mppt method for pv systems,” *IEEE Transactions on Industrial Electronics*, vol. 55, no. 7, pp. 2622–2628, July 2008.

[13] M. Fortunato, A. Giustiniani, G. Petrone, G. Spagnuolo, and M. Vitelli, “Maximum power point tracking in a one-cycle-controlled single-stage photovoltaic inverter,” *IEEE Transactions on Industrial Electronics*, vol. 55, no. 7, pp. 2684–2693, July 2008.

[14] R. Gules, J. D. P. Pacheco, H. L. Hey, and J. Imhoff, “A maximum power point tracking system with parallel connection for pv stand-alone applications,” *IEEE Transactions on Industrial Electronics*, vol. 55, no. 7, pp. 2674–2683, July 2008.

[15] J. M. Kwon, B. H. Kwon, and K. H. Nam, “Three-phase photovoltaic system with three-level boosting mppt control,” *IEEE Transactions on Power Electronics*, vol. 23, no. 5, pp. 2319–2327, Sept 2008

[16] Y. M. Chen, H. C. Wu, Y. C. Chen, K. Y. Lee, and S. S. Shyu, “The ac line current regulation strategy for the grid-connected pv system,” *IEEE Transactions on Power Electronics*, vol. 25, no. 1, pp. 209–218, Jan 2010.

[17] R. Ramaprabha, V. Gothandaraman, K. Kanimozhi, R. Divya, and B. L. Mathur, “Maximum power point tracking using ga-optimized artificial neural network for solar pv system,” in *Electrical Energy Systems (ICEES), 2011 1st International Conference on*, Jan 2011, pp. 264–268.

[18] G. C. Hsieh, H. I. Hsieh, C. Y. Tsai, and C. H. Wang, “Photovoltaic power-incrementaided incremental-conductance mppt with two-phased tracking,” *IEEE Transactions on Power Electronics*, vol. 28, no. 6, pp. 2895–2911, June 2013.

[19] S. K. Kollimalla and M. K. Mishra, “Variable perturbation size adaptive p amp;o mppt algorithm for sudden changes in irradiance,” *IEEE Transactions on Sustainable Energy*, vol. 5, no. 3, pp. 718–728, July 2014.

[20] F. Paz and M. Ordonez, “Fast and efficient solar incremental conductance mppt using lock-in amplifier,” in *2015 IEEE 6th International Symposium on Power Electronics for Distributed Generation Systems (PEDG)*, June 2015, pp. 1–6.

[21] "TP250 series". [Online]. Available: http://www.enfsolar.com/pv/panel-datasheet/Polycrystalline/19739. Accessed: 20-06-2016

[22] J. A. Gow and C. D. Manning, “Development of a photovoltaic array model for use in power-electronics simulation studies,” *IEE Proceedings - Electric Power Applications*, vol. 146, no. 2, pp. 193–200, Mar 1999.

[23] K. Nishioka, N. Sakitani, Y. Uraoka, and T. Fuyuki, “Analysis of multicrystalline silicon solar cells by modified 3-diode equivalent circuit model taking leakage current through periphery into consideration,” *Solar Energy Materials and Solar Cells*, vol. 91, no. 13, pp. 1222 – 1227, 2007.

[24] C. Carrero, J. Amador, and S. Arnaltes, “A single procedure for helping {PV} designers to select silicon {PV} modules and evaluate the loss resistances,” *Renewable Energy*, vol. 32, no. 15, pp. 2579 – 2589, 2007.

[25] T. Tan, D. S. Kirschen, and N. Jenkins, “A model of pv generation suitable for stability analysis,” *IEEE Transactions on Energy Conversion*, vol. 19, no. 4, pp. 748–755, Dec 2004.

[26] N. D. Benavides and P. L. Chapman, “Modeling the effect of voltage ripple on the power output of photovoltaic modules,” *IEEE Transactions on Industrial Electronics*, vol. 55, no. 7, pp. 2638–2643, July 2008.

[27] G. Walker, “Evaluating mppt converter topologies using a matlab pv model,” *Journal of electrical and electronics engineering, Australia*, vol. 1, pp. 138–143, January 2000.

[28] Y.-C. Kuo, T.-J. Liang, and J.-F. Chen, “Novel maximum-power-point-tracking controller for photovoltaic energy conversion system,” *IEEE Transactions on Industrial Electronics*, vol. 48, no. 3, pp. 594–601, Jun 2001.

[29] M. G. Villalva, J. R. Gazoli, and E. R. Filho, “Comprehensive approach to modeling and simulation of photovoltaic arrays,” IEEE Trans. Power Electron., vol. 24, no. 5, pp. 1198-1208, May 2009.